J|A|C|S ARTICLES

Published on Web 02/01/2010

Rapid Separation and Purification of Nanoparticles in Organic Density Gradients

Lu Bai, Xiuju Ma, Junfeng Liu, Xiaoming Sun,* Dongyuan Zhao, and David G. Evans

State Key Laboratory of Chemical Resource Engineering, P.O. Box 98, Beijing University of Chemical Technology, Beijing 100029, P. R. China

Received November 4, 2009; E-mail: sunxm@mail.buct.edu.cn

Abstract: Nanoseparation and concomitant purification of nanoparticles by ultracentrifugation in a nonhydroxylic organic density gradient has been demonstrated by separating several typical colloidal nanoparticles, including Au, Ag, and CdSe. Successful separation of Au nanowires from their spherical counterparts showed that colloidal particles can be separated not only by size but also morphology. In addition to extending the range of colloidal systems which can be separated and providing monodisperse samples that cannot be obtained by synthesis optimization alone, this method simplifies the postsynthesis treatment process and facilitates subsequent bulk assembly of the monodisperse colloids. Dissolution of organic polymers in the gradient medium both enhances the separation efficiency and also allows the direct fabrication of functional composite films with discrete monodisperse nanoparticles embedded inside.

Introduction

Nanoseparation is attracting more and more interest as an important and effective complementary process to synthesis optimization for providing strictly monodisperse nanoparticles (NPs) for investigations of their size- or shape-dependent properties.[1−7] A variety of separation methods, including magnetic separation,[3] selective precipitation,[1] filtration/diafiltration,[2,4] electrophoresis,[5] and chromatographic methods[6,7] have been explored as different ways of attaining particle fractions with ultranarrow shape and size distributions. The density gradient ultracentrifugation method—a general, nondestructive and scalable separation method adapted from biomacromolecular separation technology[8]—has recently demonstrated its high potential for sorting colloidal NPs according to their chemical, structural, and size differences.[9−16] However, up to now, most ultracentrifugation separation work has focused on aqueous density gradients and there have been few attempts to separate organic-soluble functional NPs obtained by nonhydroxylic synthetic routes. These have shown high potential for large scale industrial production and application,[17−19] and hence developing effective means for their separation is a key objective if progress in this rapidly growing field is to be maintained.

Here we report the separation of colloidal NPs dispersed in nonhydroxylic solvents using ultracentrifugation in an organic density gradient which gives rapid separation and concomitant purification. In addition to extending the range of colloidal systems which can be separated, we found there are several other advantages of using an organic density gradient rather than the conventional aqueous gradients. First, combining synthesis optimization and separation can afford samples that cannot be provided by synthesis optimization alone. Second, colloidal NPs synthesized and dispersed in an organic medium can be directly separated after synthesis without transfer to an aqueous medium, which avoids the possible aggregation and clustering of NPs under nonoptimized conditions. Third, since the density gradients are composed of organic solvents without any solid additives, the solvents can be evaporated without leaving any residue, facilitating bulk assembly of the resulting monodisperse colloids after fractionation. Last and by no means least

(1) McLeod, M. C.; Anand, M.; Kitchens, C. L.; Roberts, C. B. *Nano Lett.* **2005**, *5*, 461–465.
(2) Akthakul, A.; Hochbaum, A. I.; Stellacci, F.; Mayes, A. M. *Adv. Mater.* **2005**, *17*, 532–535.
(3) Yavuz, C. T.; Mayo, J. T.; Yu, W. W.; Prakash, A.; Falkner, J. C.; Yean, S.; Cong, L.; Shipley, H. J.; Kan, A.; Tomson, M.; Natelson, D.; Colvin, V. L. *Science* **2006**, *314*, 964–967.
(4) Sweeney, S. F.; Woehrle, G. H.; Hutchison, J. E. *J. Am. Chem. Soc.* **2006**, *128*, 3190–3197.
(5) Hanauer, M.; Pierrat, S.; Zins, I.; Lotz, A.; Sonnichsen, C. *Nano Lett.* **2007**, *7*, 2881–2885.
(6) Krueger, K. M.; Al-Somali, A. M.; Falkner, J. C.; Colvin, V. L. *Anal. Chem.* **2005**, *77*, 3511–3515.
(7) Tu, X.; Zheng, M. *Nano Res.* **2008**, *1*, 185–194.
(8) Price, C. A. *Centrifugation in Density Gradients*; Academic Press: New York, 1982; Chapter *5*.
(9) Arnold, M. S.; Green, A. A.; Hulvat, J. F.; Stupp, S. I.; Hersam, M. C. *Nat. Nanotechnol.* **2006**, *1*, 60–65.
(10) Arnold, M. S.; Stupp, S. I.; Hersam, M. C. *Nano Lett.* **2005**, *5*, 713–718.
(11) Jamison, J. A.; Krueger, K. M.; Yavuz, C. T.; Mayo, J. T.; LeCrone, D.; Redden, J. J.; Colvin, V. L. *ACS Nano* **2008**, *2*, 311–319.
(12) Fagan, J. A.; Becker, M. L.; Chun, J.; Hobbie, E. K. *Adv. Mater.* **2008**, *20*, 1609–1613.
(13) Chen, G.; Wang, Y.; Tan, L. H.; Yang, M.; Tan, L. S.; Chen, Y.; Chen, H. *J. Am. Chem. Soc.* **2009**, *131*, 4218–4219.
(14) Sun, X. M.; Zaric, S.; Daranciang, D.; Welsher, K.; Lu, Y. R.; Li, X. L.; Dai, H. J. *J. Am. Chem. Soc.* **2008**, *130*, 6551–6555.
(15) Sun, X. M.; Liu, Z.; Welsher, K.; Robinson, J. T.; Goodwin, A.; Zaric, S.; Dai, H. *Nano Res.* **2008**, *1*, 203–212.
(16) Sun, X. M.; Tabakman, S. M.; Seo, W.-S.; Zhang, L.; Zhang, G.; Sherlock, S.; Bai, L.; Dai, H. *Angew. Chem., Int. Ed.* **2009**, *48*, 939–942.
(17) Jun, Y.-w.; Choi, J.-s.; Cheon, J. *Angew. Chem., Int. Ed.* **2006**, *45*, 3414–3439.
(18) Wang, X.; Li, Y. D. *Chem. Commun.* **2007**, 2901–2910.
(19) Yin, Y. D.; Alivisatos, A. P. *Nature* **2005**, *437*, 664–670.

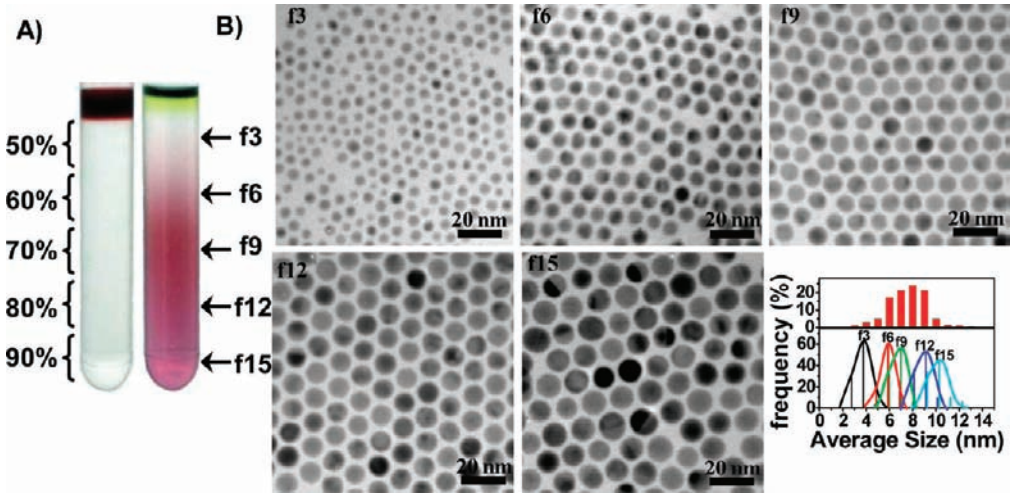

Figure 1. (A) Digital images of ultracentrifuge vessels containing Au nanoparticles before (left vessel) and after (right vessel) separation at 25000 rpm for 12 min. (B) TEM images of typical fractions. The graph in the bottom right corner shows a comparison of the size distribution difference before (red columns in the upper section) and after (colored columns in the lower section) centrifugation separation. Each size histograms was measured from at least 200 particles.

important, a third component—typically an organic polymer such as polystyrene (PS)—can be dissolved as part of the gradient medium. Colloidal NPs with focused size distribution can thus be captured in the gradient together with polymers, and these fractions can be fabricated into functional composite films with discrete NPs embedded inside by vaporizing the solvent. In this paper, we demonstrate the above features by separating several typical colloidal functional metal (Au, Ag) and semiconductor (CdSe) NPs with different shape and size ranges.

Results and Discussion

The first sample employed to demonstrate the separation efficacy was Au NPs synthesized following the reported method.[20] The principles and experimental details of the separation methodology can be found in our previous reports[14−16] (and the Supporting Information, SI), but the gradient-making materials used here are nonpolar organic solvents, cyclohexane and tetrachloromethane, rather than water as used in our previous work. In brief, a thin layer (usually 0.1−0.4 mL) of the Au colloidal suspension to be separated is floated on a density gradient made by mixing different ratios of cyclohexane and tetrachloromethane (50−90% of CCl_4 by volume; density range, 1.13−1.41 g/cm^3), as labeled beside the centrifuge vessel shown in Figure 1A. It should be stressed that no preliminary purification is necessary prior to the gradient separation: the Au colloidal suspension is used directly after synthesis, and hence contains impurities like oleylamine. As the suspended Au particles (Au concentration: ∼1 mg/mL) are well wrapped and isolated by oleylamine, they can be considered as sedimenting ideally as discrete entities during the subsequent centrifugation. Particles with a given sedimentation rate, which is determined by size and shape for a given material, travel down the centrifuge vessel as a separate zone. When the sedimentation is stopped before the particles reach their density equilibria by removing the centrifugal force, the particles are captured and sorted along the vessel. Here we centrifuged at 25000 rpm (∼80000*g*) for 12 min. Figure 1B shows that the yellow colored reaction solution containing oleylamine was retained at the top of gradient because of its low molecular weight, while Au NPs moved to subsequent layers. Samples for TEM were made by directly drying individual separated fractions on carbon films on copper grids. The clear images obtained are evidence for purification having been achieved, since impurities such as oleylamine would result in blurred images if present. TEM results of fraction 3 (labeled as "f3" in Figure 1B) contained ∼4.8 nm Au NPs. The average particle diameter of subsequent fractions (f6, f9, f12, and f15) gradually increased from 7.2, 8.0, 9.3 to 10.9 nm, respectively. The size deviation was usually <1.5 nm as indicated by the histograms of particle size (see SI, Figure S1). Since there are thousands of organic solvents with tunable polarity and solubility that can be used for generating density gradients, as long as they are miscible with the NP concerned and possess different density, separation using organic density gradients significantly widens the range of applicable colloidal NP systems.

It is well-known that the sedimentation speed of the particles increases as the centrifugal force increases. Thus, more rapid separation can be achieved by simply increasing centrifugation speed. As an example, we separated the same batch of Au NPs as in Figure 1 using a reduced centrifugation time (5 min) by increasing the centrifugation speed to 50000 rpm (∼330000*g*, Figures S2 and S3 in the SI) with the same density gradient. The method can also be extended to the separation of Ag NPs (Ag concentration: ∼1.1 mg/mL), but since they possesses lower mass density than Au but similar size, the centrifugation time had to be extended to 8 min (Figures S4 and S5 in the SI) to afford similar distributions along the centrifugation vessel.

NPs can be separated not only by size, but also by shape because the latter influences the ratio of mass to frictional constant, which is one of the key factors affecting the terminal velocity.[21] This provides an opportunity to obtain samples with distinctive shapes that are difficult to prepare in a "pure" form by synthesis optimization alone. Sub-2 nm diameter Au nanowires (NWs) are generally obtained as a mixture containing Au NPs.[22] Ultracentrifuge separation can separate these two com-

(20) Liu, J.; Chen, W.; Liu, X.; Zhou, K.; Li, Y. *Nano Res.* **2008**, *1*, 46–55.
(21) Brakke, M. K. *J. Am. Chem. Soc.* **1951**, *73*, 1847–1848.
(22) Huo, Z.; Tsung, C.-k.; Huang, W.; Zhang, X.; Yang, P. *Nano Lett.* **2008**, *8*, 2041–2044.

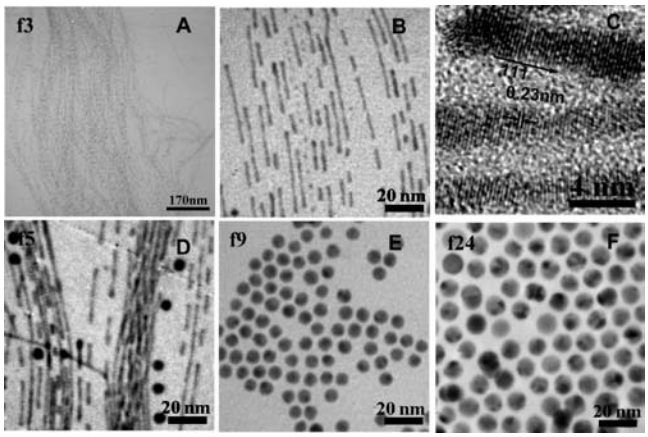

Figure 2. Typical TEM images of (A−C) separated ultrathin Au nanowires in f3 and (D) f5, and nanoparticles separated in (E) f9 and (F) f24.

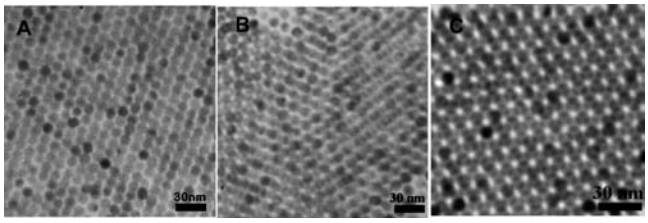

Figure 3. Typical TEM images of self-assembled monodisperse Au nanoparticles with size range of (A) 8.7 ± 1 nm and (B, C) 12.0 ± 1 nm.

ponents (Au concentration: ∼1 mg/mL) because the high aspect ratio of the NWs leads to them experiencing much higher friction than the spherical NPs, and they were thus captured in the upper layer (f3) (Figure 2A−C). The next layer (f5) contained a majority of nanowires, but with some small NPs (Figure 2D). Following the transitional layer, monodisperse spherical NPs appeared and were sorted according to size in the subsequent layers (Figure 2E,F).

One of the features of monodisperse NPs is their capability to self-assemble into superstructures. We demonstrate this by assembly into an Au NP thin film at the interface of a good solvent (cyclohexane) and antisolvent (ethanol)[23] after separation. The setup is shown in Figure S6 in the SI. Ethanol was injected beneath a cyclohexane solution of Au NPs, thus raising it up. As diffusion of ethanol into the cyclohexane layer proceeded, the Au NPs near the cyclohexane−ethanol interface clustered and aggregated to form a monolayer NP film. This is a common observation for monodisperse NPs with different size ranges, and results in close packed hexagonal superlattices (Figure 3A−C). Forming films by such close packing provides new opportunities for using the materials in sensing or other optical property investigations.[24]

To make the separation more visible, CdSe NPs (CdSe concentration: ∼25 mg/mL), which are well-known for their size-dependent fluorescence,[25] were synthesized[26] and separated using the cyclohexane + tetrachloromethane gradient. Figure 4A shows photographs of the centrifuge vessel under white light (left) and irradiation by 365 nm UV light (right). Since the fluorescence of CdSe NPs depends on their size, the different colored bands observed along the vessel are evidence of size separation, as larger nanocrystals with more red-shifted emissions were observed at lower positions of the separation column. High resolution transmission electron microscopy (HRTEM) gave direct evidence which confirmed the size separation (Figure 4).

Polystyrene (PS), as a typical polymer, was introduced into the cyclohexane + tetrachloromethane gradient to make a polymer-containing density gradient and to further assist in the separation of oleic acid-wrapped CdSe NPs (CdSe concentration: ∼25 mg/mL). It can be clearly seen that the bands in the PS-containing gradient showed much more limited movement (Figure 5A-II) than in the absence of PS (Figure 5A-I) after 60 min centrifugation at 50000 rpm (∼330000*g*). This suggests that PS slowed down the sedimentation of CdSe NPs by increasing the viscosity of the layers. The CdSe NPs reached essentially the same separation as in Figure 5A-I when the centrifugation time was almost doubled (110 min, Figure 5A-III). The colored bands were transferred to plastic vials (see Figure S7 in the SI,) and used for subsequent fluorescence measurements (Figure 5B,C).

Optical fluorescence spectra from various zones along the vessel were clearly increasingly red-shifted on descending the vessel, quantitatively confirming the size evolution. The original CdSe solution showed a wide (>100 nm) fluorescence spectrum (the black lines in Figure 5B,C) with two peaks around 450 and 550 nm. The 450 nm peak results from oleic acid, as can be seen by comparison with the spectrum of a solution of oleic acid in cyclohexane (curve OA in Figure 5B,C). The increasing red shift is observed throughout the successive fractions of the PS-containing gradient (Figure 5C, as seen for the pairs of curves labeled in the same colors; please refer to Figure 5A for fraction number labeling), but the discrimination effect is lost in the last few fractions in the absence of PS (Figure 5B, as labeled with the same colors of lines). The fluorescence spectra of most fractions are typically ∼50 nm in width at half peak height, while the lowest fractions in the gradient without PS (e.g., f32 in Figure 5B), showed peaks as wide as 90 nm. This might be caused by clustering of large and small NPs, or droplet sedimentation,[27] which disturbed the separation. The absence of such mixing effects in the PS-containing gradient suggests that PS-incorporation enhances the separation, possibly by stabilizing the gradient layers and declustering the NPs.

In addition to enhancing the separation efficiency, the addition of polymers also offers the possibility of directly fabricating composite films with monodisperse and discrete NPs embedded inside them. We show here how fractions containing both PS and monodisperse CdSe NPs with different size ranges were transformed into colorful composite films after driving off the cyclohexane and tetrachloromethane. Since the liquid can be filled into any preformed template, such as the concave rectangular grooves on a polymer film (Figure 5D), colorful words or patterns can be written using the fractions as different colored inks. The as-formed films are highly flexible (Figure S7C in the SI), highlighting their potential applications in labeling, panel display, and information technology.

Further investigation indicated that the full width at the half peak (FWHP) in the spectra of fractions can be reduced to as

(23) Xie, T.; Li, S.; Peng, Q.; Li, Y. *Angew. Chem., Int. Ed.* **2009**, *48*, 196–200.
(24) Tao, A. R.; Huang, J.; Yang, P. *Acc. Chem. Res.* **2008**, *41*, 1662–1673.
(25) Murray, C. B.; Norris, D. J.; Bawendi, M. G. *J. Am. Chem. Soc.* **1993**, *115*, 8706–8715.
(26) Yang, Y. A.; Wu, H.; Williams, K. R.; Cao, Y. C. *Angew. Chem., Int. Ed.* **2005**, *44*, 6712–6715.
(27) Brakke, M. K.; Daly, J. M. *Science* **1965**, *148*, 387–389.

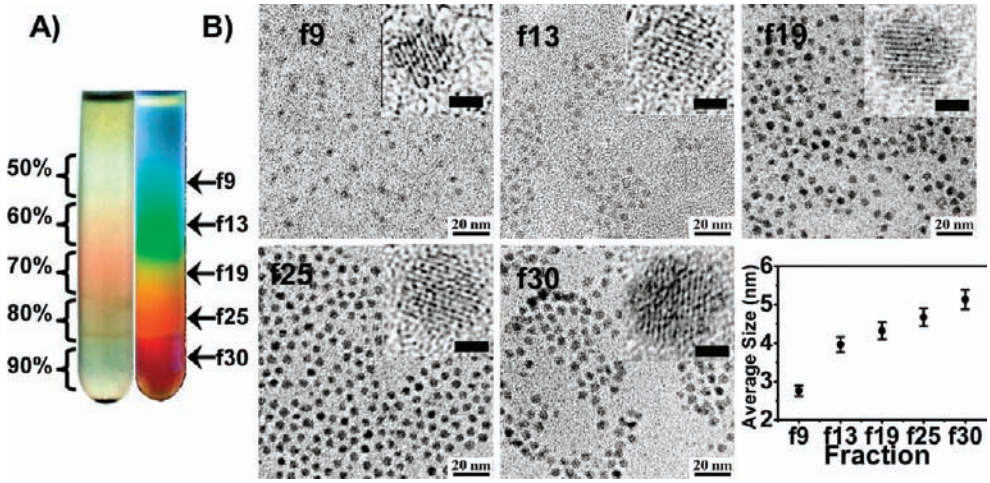

Figure 4. (A) Digital camera images of ultracentrifuge vessels containing CdSe nanoparticles using a cyclohexane + tetrachloromethane gradient after separation at 50000 rpm for 60 min. The left image was recorded under white light; the right image was recorded under UV irradiation at 365 nm. (B) HRTEM images of typical CdSe nanoparticle fractions. Magnified individual nanoparticles are shown in the insets (the bars in the insets are 2 nm). The graph in the bottom right corner shows the size evolution of particles along the centrifuge vessel.

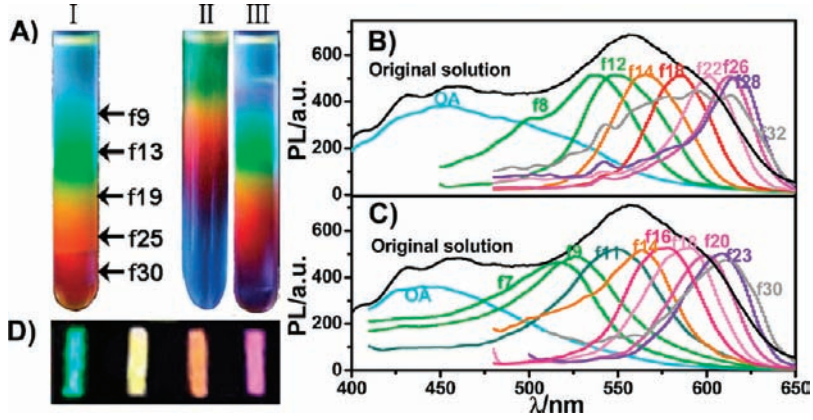

Figure 5. (A) Digital camera images of ultracentrifuge vessels containing CdSe NPs: (vessel I) PS-free gradient, 60 min centrifugation at 50000 rpm; (vessel II) PS-containing gradient, 60 min centrifugation at 50000 rpm; and (vessel III) PS-containing gradient, 110 min centrifugation at 50000 rpm. All images were recorded under UV irradiation at 365 nm. (B) Fluorescence spectra of typical fractions obtained from vessel I, PS-free gradient. (C) Fluorescence spectra of fractions obtained from vessel III, PS-containing gradient. (D) Digital image of composite strips converted from PS-containing fractions of CdSe NPs with different sizes, recorded under UV irradiation at 365 nm (size: 105 mm × 20 mm).

low as 30 nm, using the same strategy and a "green" CdSe sample with initial FWHP of 50 nm as the starting sample (see Figure S8 in the SI). The above results demonstrate the versatility and efficacy of our NP separation method. Although there have been many reports of the synthesis of relatively monodisperse NPs, when the target NPs are extremely small (<10 nm), even sub-1 nm deviations in size result in significant polydispersity. In such cases, postsynthesis size separation is essential since the required monodispersity cannot be achieved by synthesis optimization alone.

For practical purposes, it will be necessary to scale-up the process described here for the separation of NPs. In conventional biomacromolecular separations, the reorienting gradient rotor principle[28]—in which a static gradient is reoriented into a radial configuration during acceleration and is subsequently recovered in its original orientation at rest—makes feasible the construction of high-speed, large-volume rotors suitable for scale-up of separations and the same approach should be applicable to the separation of NPs using an organic density gradient. Such work is currently underway in our laboratory.

Conclusion

A simple, rapid, and effective organic density gradient centrifugation method has been developed for separation and purification of nanocrystals. Colloidal NPs with different size and shape, and different chemical and physical properties, can be separated by sedimentation at different rates as long as they are dispersible in a mixture of miscible organic solvents. The separated and purified NPs can self-assemble into superlattices by selective aggregation at interfaces. Polymers can be incorporated into the gradient in order to enhance the separation and the resultant fractions can be fabricated into functional composite films by vaporizing the gradient-making solvents. Since a large number of metal and semiconductor colloidal NPs are synthesized in organic systems, the separation, purification, and transformation method described here can be employed directly on the crude product mixture and has high potential to contribute to the development of future advanced science and technology based on functional nanocrystals.

(28) Anderson, N. G.; Burger, C. L. *Science* **1962**, *136*, 646–648.

Acknowledgment. We thank Dr. Fang Sun for providing some experimental materials. This work was supported by NSFC, the 973 Program (2009CB939802) and the "111" Project (B07004), the Foundation for Authors of National Excellent Doctoral Dissertations of P. R. China, the Program for New Century Excellent Talents in Universities, and the Project sponsored by the Scientific Research Foundation for Returned Overseas Chinese Scholars (SRF for ROCS), State Education Ministry (SEM).

Supporting Information Available: Detailed experimental procedures for the synthesis, separation, and assembly of the nanoparticles; quantitative data of the separation of Au, Ag, and CdSe NPs; photograph of the experimental setup for the self-assembling of Au NPs. This material is available free of charge via the Internet at http://pubs.acs.org.

JA908971D